

# Structural, Dielectric and Mössbauer Properties of $Mg_{0.2}Mn_{0.5}Ni_{0.3}Al_yFe_{2-y}O_4$ Nanoferrites Prepared by Citrate Precursor Method

Satish Verma, Jagdish Chand, Pooja Dhiman, Sarveena and M. Singh

Department of Physics, Himachal Pradesh University, Summer-Hill, Shimla-171005, INDIA.

Email: satishapurva@gmail.com

## Abstract

Polycrystalline  $Mg_{0.2}Mn_{0.5}Ni_{0.3}Al_yFe_{2-y}O_4$  ( $y=0.0-0.10$ ) nanoferrites were prepared by citrate precursor method. Particle size decreases from 102.25 nm to 41.65 nm with increasing  $Al^{3+}$  ions concentration. The unit cell parameter 'a' is found to decrease linearly with  $Al^{3+}$  ions due to its smaller ionic radius. Theoretical lattice parameter ' $a_{th}$ ', volume 'V' of the unit cell, oxygen positional parameter 'u', ionic radii of A-site and B-site were determined.  $^{57}Fe$  Mössbauer measurements performed at room temperature shows a six line pattern for sample with larger particle size and a doublet pattern for sample with smaller particle size, owing to weakening of magnetic exchange interaction, which is indicative of their super paramagnetic nature. Dielectric constant and dielectric loss were determined in the frequency range 0.075 MHz – 30 MHz. Dielectric behaviours have been attributed to the Maxwell-Wagner type interfacial polarization.

## 1. Introduction

The iron oxide and substituted iron oxide nanomaterials known as spinel ferrites are used for magnetic memory and magneto optical devices, as contrasting agents in magnetic resonance imaging, for refrigeration and as sensors. Spinel ferrites are still one of the basic materials of modern electronics and computers technology. When  $Fe^{3+}$  ions are replaced by  $Al^{3+}$  ions, the crystal structure becomes a cubic spinel structure. The addition of  $Al^{3+}$  ions gives interesting Mössbauer spectra and drastically changes magnetic hyperfine fields and other Mössbauer and X-ray parameters. The aim of present work is to study effect of  $Al^{3+}$  ions substitution on physical, electric and Mössbauer properties of  $Mg_{0.2}Mn_{0.5}Ni_{0.3}Al_yFe_{2-y}O_4$  nanoferrites.

## 2. Results and Discussion

XRD pattern of  $Mg_{0.2}Mn_{0.5}Ni_{0.3}Fe_2O_4$  ferrite, Figure 1 indicate that material has a well-defined crystalline cubic single phase. Crystalline size was estimated using Scherrer's formula and it decreases from 102.25 nm to 41.65 nm with increasing  $Al^{3+}$  ions concentration.

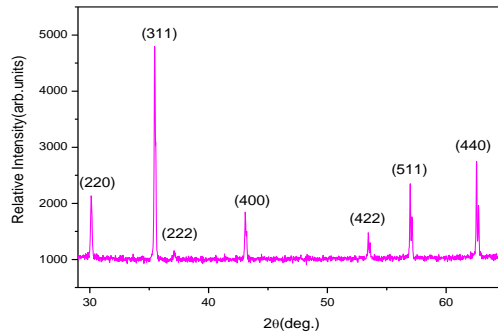


**FIGURE 1.** XRD pattern of  $Mg_{0.2}Mn_{0.5}Ni_{0.3}Fe_2O_4$  ferrite. The radii of tetrahedral and octahedral sites were calculated, Table 1, using lattice parameter 'a' and equations given by Smit and Wijn [1]:

$$R_{\text{tetra}} = \sqrt{3} (u - \frac{1}{4}) a - R_0 \quad (1)$$

$$R_{\text{octa}} = (5/8 - u) a - R_0 \quad (2)$$

Here  $R_0 = 1.32 \text{ \AA}$  is the radius of oxygen atom. Tetrahedral and octahedral site radii decrease continuously with increasing  $Al^{3+}$  ions concentration. The oxygen positional parameter and theoretical value of lattice parameter were calculated using relations [2]:

$$u = [(R_{\text{tetra}} + R_0)/a\sqrt{3} + 0.25] \quad (3)$$

$$a_{\text{th}} = 8/3\sqrt{3} [(R_{\text{tetra}} + R_0) + \sqrt{3} (R_{\text{octa}} + R_0)] \quad (4)$$

Figure 2 shows Mössbauer spectra of  $y=0.0$  and  $0.10$  at room temperature. For  $y=0.0$ , Mössbauer spectrum exhibits a superposition of two Zeeman sextets, one sextet correspond to higher magnetic field attributed to  $Fe^{3+}$  ions on B-site, and other sextet correspond to lower magnetic field attributed to  $Fe^{3+}$  ions on A-site. Mössbauer spectra of  $y=0.10$  is characterized by simultaneous presence of central paramagnetic doublet.

The difference between the paramagnetic and the ferromagnetic behaviour can be explained by super paramagnetic relaxation time ' $\tau$ ', using equation:

$$\tau = \tau_0 \exp (KV/k_B T) \quad (5)$$

Magnetic sextets corresponds to ferromagnetic particles of larger size and for these particles ( $\tau > \tau_{\text{obs}}$ ). When  $\tau$  is less than Larmor precession time  $\tau_{\text{obs}}$  i.e. ( $\tau < \tau_{\text{obs}}$ ) a super paramagnetic doublet is observed in Mössbauer

**TABLE 1.** Structural parameters of ferrite samples.

y	a(Å)	a <sub>th</sub> (Å)	(Å) <sup>3</sup>	R <sub>tetra</sub>	R <sub>octa</sub>	u (Å)
0.0	8.399	8.397	592.53	0.5849	0.7294	0.3808
0.05	8.394	8.393	591.58	0.5860	0.7305	0.3807
0.10	8.390	8.388	590.71	0.5914	0.7364	0.3809

spectrum. Presence of doublet alone in the Mössbauer spectra can be attributed to super paramagnetic relaxation due to extremely small size of crystallites [3].

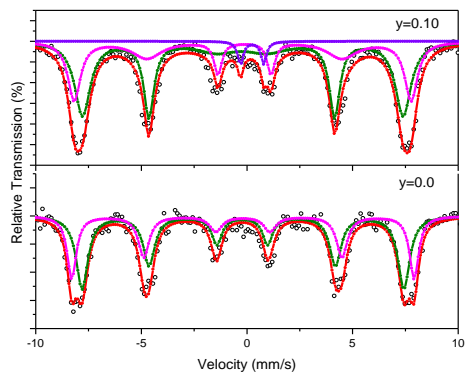


**FIGURE 2.** Mössbauer spectra of  $Mg_{0.2}Mn_{0.5}Ni_{0.3}Al_yFe_{2-y}O_4$  ferrite samples.

There is no significant change in the values of isomer shift corresponding to  $Fe^{3+}$  ions at A- and B-sites with an increase in  $Al^{3+}$  ions concentration. This indicates that there is negligible influence on the 's' electron charge density around  $Fe^{3+}$  nuclei at both the sites. Quadrupole interaction has values close to zero for A-site and B-site. The hyperfine magnetic field at A-site and B-site shows a gradual decrease with increasing  $Al^{3+}$  ions concentration. This can be explained on the basis of super transferred hyperfine field at central cation which originates from magnetic moments of nearest-neighbour cations. The introduction of  $Al^{3+}$  ions, which replaces  $Fe^{3+}$  ions from the B-site decreases intra-sub lattice contributions, which in turn decreases hyperfine magnetic field. Net magnetic field is due to dominant  $Fe^{3+}_A - O^{2-} - Fe^{3+}_B$  linkage, because A-B interaction is stronger than A-A and B-B interactions. The distribution of  $Fe^{3+}$  ions amongst the A- and B-sublattices can be understood from the relation between the area ratio of B- to A-sites subspectra and (molar ratio) y, Table 2. The decrease of this ratio against y indicate that the substitution process often reduces the  $Fe^{3+}$  ions number in the lattice at the expense of the number of  $Fe^{3+}$  ions at the B sublattice.

Figure 3 shows the variation of dielectric constant and dielectric loss with frequency at different temperature of y=0.0. There is initial decrease in dielectric constant and dielectric loss with frequency followed by appearance of the resonance which may be due to matching of frequency of charge transfer between  $Fe^{2+} - Fe^{3+}$  ions and that of applied electric field. Dielectric constant of any material in general is due to dipolar, electronic, ionic and interfacial polarizations.

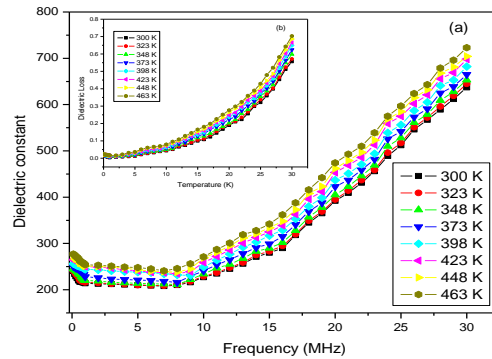


**FIGURE 3.** Variation of (a) dielectric constant (b) dielectric loss (inset) with frequency at different temperature of  $y=0.0$ .

**TABLE 2.** Mössbauer and dielectric parameters.

Samples	Area ratio B/A	$(\epsilon')$ 1MHz	$(\epsilon'')$ 1 MHz ( $\times 10^{-3}$ )	Tan $\delta$ $\epsilon''/\epsilon'$ ( $\times 10^{-5}$ )	Q-Factor
$y = 0.0$	0.710	214	3.9	1.822	0.548
$y = 0.05$	0.556	207	1.9	0.917	1.090
$y=0.10$	0.492	202	1.3	0.643	1.555

At low frequencies, dipolar and interfacial polarizations are known to play most important role. Both these polarizations are strongly temperature dependent. At high frequencies, electronic and ionic polarizations are main contributors and their temperature dependence is insignificant. Figure 3 [Inset], shows that dielectric loss decreases initially with increasing frequency which can be explained on the basis of Koops' phenomenological model [2,4], followed by appearance of a resonance with peak occurring at frequencies higher than 30 MHz.

### Conclusions

Mössbauer spectra exhibit broad doublet with increasing  $Al^{3+}$  ions concentration which suggest super paramagnetic nature and collapse of long range ferromagnetic ordering due to smaller particle size. Very low dielectric losses even at high frequencies make these materials suitable for microwave applications.

### References

- [1] Satish Verma, J. Chand, K. M. Batoo and M. Singh, J. Alloys. Compd. **565**, 148-153 (2013).
- [2] Satish Verma, Jagdish Chand and M. Singh, J. Alloys. Compd. **587**, 763-770 (2014).
- [3] Satish Verma, Jagdish Chand, Khalid Mujasum Batoo and M. Singh, J. Alloys. Compd. **551**, 715-721 (2013).
- [4] C. G. Koops, Phys. Rev. **83**, 121-124 (1951).